JACS Au
AN OPEN ACCESS JOURNAL OF THE AMERICAN CHEMICAL SOCIETY

Editors' Choice
Open Access

pubs.acs.org/jacsau

Letter

In Vivo Optogenetic Manipulation of Transgene Expression in Retinal Neurovasculature

Eric Brandhorst, Liang Xu, Maxime Klimezak, Bastien Goegan, Huixiao Hong, Hans-Peter Hammes, Alexandre Specht,* and Sidney Cambridge*

Cite This: *JACS Au* 2024, 4, 2818–2825

Read Online

ACCESS | Metrics & More | Article Recommendations | Supporting Information

ABSTRACT: The retina is prone to developing pathological neovascularization, a leading cause of blindness in humans. Because excess neovascularization does not affect the entire retina, global inhibition treatment of angiogenesis critically interferes with healthy, unaffected retinal tissue. We therefore established an *in vivo* photoactivated gene expression paradigm which would allow light-mediated targeting of antiangiogenic genetic treatment only to affected retinal regions. We synthesized a "caged" (*i.e.*, reversibly inhibited) photosensitive 4-hydroxytamoxifen analog. Molecular docking analyses validated its reduced transcriptional activity. Caged 4-hydroxytamoxifen was intravitreally injected into mice harboring the inducible Cre/lox system, with CreERT2 being expressed *via* the Tie2 promoter in the neurovasculature. Subsequent *in vivo* irradiation of eyes significantly induced retinal expression of a Cre-dependent transgene in retinal blood vessels. Using GFAP-CreERT2 mice, successful photoactivation was also achieved in eyes and also in *ex vivo* brain slices for validation of the approach. This highlights the possibility of light-mediated gene therapies specific for the retina, a key first step in personalized medicine.

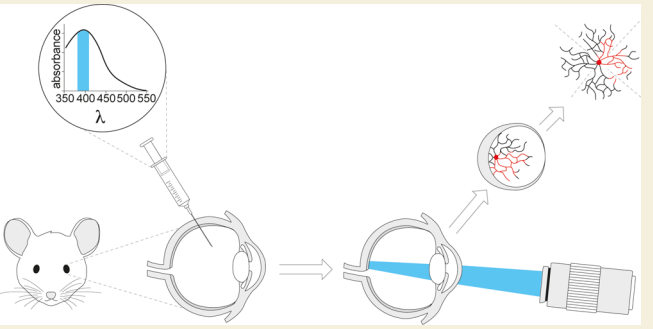

KEYWORDS: *retina, photoactivated gene expression, caged compounds, Cre/lox system, vascularization*

Degeneration of the retinal vasculature is a leading cause for human blindness worldwide. Pathological neovascularization occurs in diseases such as diabetic retinopathy, with a phenotype of excess, potentially unstable, and leaky blood vessels causing a cascade of reactions in affected retinas which ultimately can lead to severe vision impairment. Current attempts to block further vascularization as the disease phenotype progresses are typically based on blocking vascular endothelial growth factor (VEGF) pathways, either by antibodies against VEGF or by gene therapies.[1] In mouse animal models and in humans, such approaches showed promising results.[2] However, all of these treatments are global in nature and affect the entire eye, *i.e.*, pathological *and* healthy retinal tissue. Because VEGF also exhibits critical neuroprotective and neurotrophic functions,[3,4] it is imperative to develop treatments that can be spatially restricted to the pathological regions in the retina. To address this, we decided to develop a light-sensitive gene expression paradigm for eyes *in vivo*. The future goal was to be able to restrict transgene expression, such as anti-VEGF binding molecules, to defined pathological regions of the eye by irradiation with light. "Optogenetic" or photoactivated gene expression was first demonstrated more than two decades ago with a light-sensitive transcription factor protein.[5] More recently, conditional gene expression methods such as the inducible Tet system were rendered light-sensitive by reversible modification of small-molecule inducers with a light-sensitive (*i.e.*, photoremovable) protecting group, also called a "caging" group.[6,7] Photoactivated transgene expression was successfully demonstrated in organotypic hippocampal slices[8] and zebrafish.[9] As a proof of principle, in this work we demonstrated photoactivated transgene expression in retinas of living eyes (Figure 1). For this, we synthesized a light-sensitive analog of 4-hydroxytamoxifen (also called Afimoxifene) to allow tight cell-type-specific control of transgene expression with the Cre/lox system.[10,11] Administration of caged 4-hydroxytamoxifen to the eyes of Cre/lox mice followed by irradiation allowed optogenetic induction of the reporter gene tdTomato in blood vessel cells of the retina.

RESULTS

4-Hydroxytamoxifen (4-OHT, **2**) is an active metabolite of tamoxifen able to specifically control transgene expression

Received: May 14, 2024
Revised: May 27, 2024
Accepted: June 14, 2024
Published: July 15, 2024

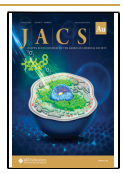

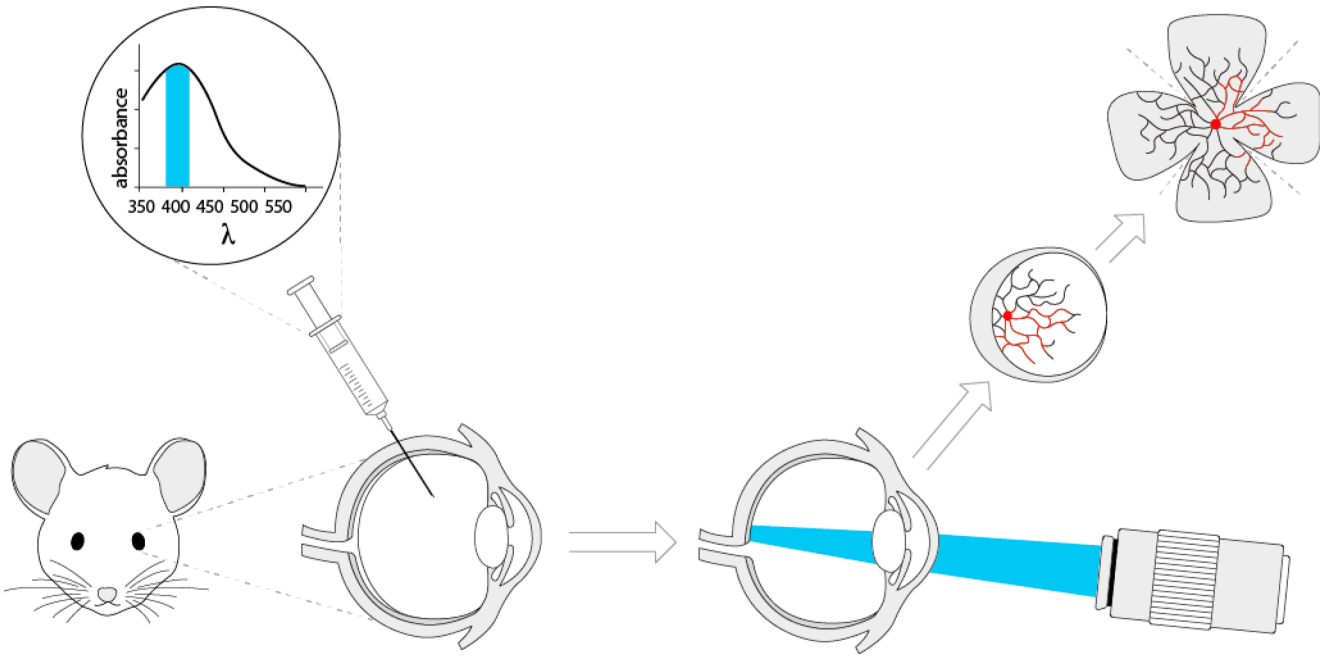

Figure 1. Illustration of the *in vivo* photoactivation approach for retinal transgene expression.

through the inducible Cre/lox system.[10] For optogenetic manipulation of transgene expression in the living eye, it was critical to shift uncaging wavelengths to the visible range to limit phototoxicity.[12] Previous modifications of 4-OHT using *o*-nitrobenzyl[13,14] or coumarinyl[15] photoremovable protecting groups required UV irradiation under 400 nm for photolysis. During the past decade, however, breakthroughs in photosensitive protection chemistry have allowed efficient uncaging at wavelengths around 450 nm and higher.[16−18] We thus devised a new strategy for the synthesis of caged 4-OHT with optimized excitation in the visible range for *in vivo* applications. We previously developed a new photoremovable group, 2-(4′-(bis(2-(2-methoxyethoxy)ethyl)amino)-4-nitro-[1,1′-biphenyl]-3-yl)propan-1-ol (EANBP, **1**).[19] The photolytic absorption range of EANBP-caged 4-OHT was found to be between 360 and 470 nm with a peak around 400 nm (Figure 1). In the present work, the uncaging wavelength range of EANBP-caged 4-OHT provided us the flexibility to perform *in vivo* photoactivation experiments with a standard DAPI filter set (365 ± 20 nm), while future studies will be able to take advantage of its higher absorbance in the visible range around 400−420 nm. EANBP was synthesized as described[20] and was coupled to commercially available 4-OHT at the phenolic 4-OH position of tamoxifen through a carbonate linkage in order to generate EANBP-4-OHT (**3**) (Figure 2). Next, the photoinduced liberation of 4-OHT from **3** was monitored by UV−vis spectroscopy and HPLC. During photolysis at 405 nm (see Methods and Figure S1), a new broad absorbance at 485 nm appeared while the initial absorbance at 400 nm gradually diminished. The appearance of an isosbestic point at 445 nm indicated homogeneous reactions. HPLC indicated 52% photoliberation of 4-OHT (see Methods and Figure S2). The quantum yield for the **3** uncaging was assessed to be 0.16 by competition with the EANBP-GABA analog[19] as a reference molecule (see Methods and Figure S3).

In mouse brains, unmodified 4-OHT exhibited pharmacological half-lives of about 16−18 h,[21] so we considered the thermal stability of EANBP-4-OHT (18% hydrolysis after 48 h) sufficient for *in vivo* applications. Prior to using EANBP-4-OHT for photoactivated transgene expression in eyes, we verified its chemical inactivation by *in silico* modeling[22,23] and by molecular docking analyses[24] to a mutated version of the human estrogen receptor (hER). As part of the CreERT2 fusion protein, these three mutations of hER (G440V, M543A, and L544A)[25] render the inducible Cre/lox system less sensitive to endogenous estradiol. A negative binding value for 4-OHT of −9.5 kcal/mol indicated a high affinity to the mutated hER, while the positive binding energy for EANBP-4-OHT (0.9 kcal/mol) confirmed that the caged compound could not bind to the relevant ligand-binding domain (Figure 3).

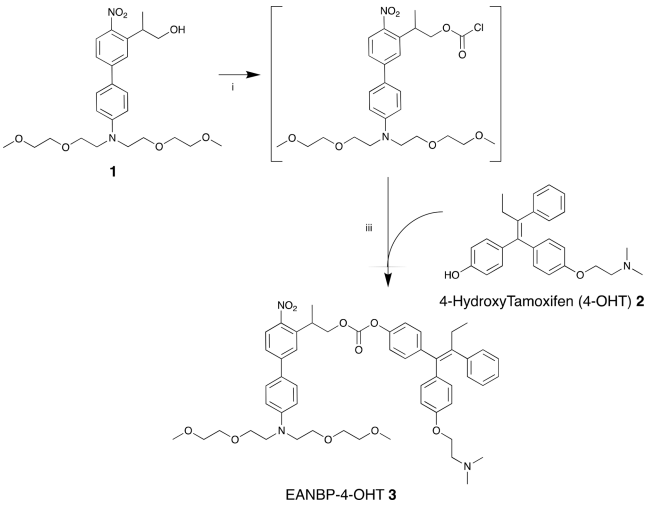

Figure 2. Synthesis of EANBP-4-OHT. Reagents and conditions: (i) triphosgene, DIPEA, THF, 0 °C, 3 h, not purified; (ii) DMAP, CH_2Cl_2, reflux, 19 h, 20% over two steps.

We verified the suitability of EANBP-4-OHT for photoactivated gene expression in *ex vivo* hippocampal brain slices.[26] We used double transgenic mice expressing (i) the mutated

https://doi.org/10.1021/jacsau.4c00434
JACS Au 2024, 4, 2818−2825

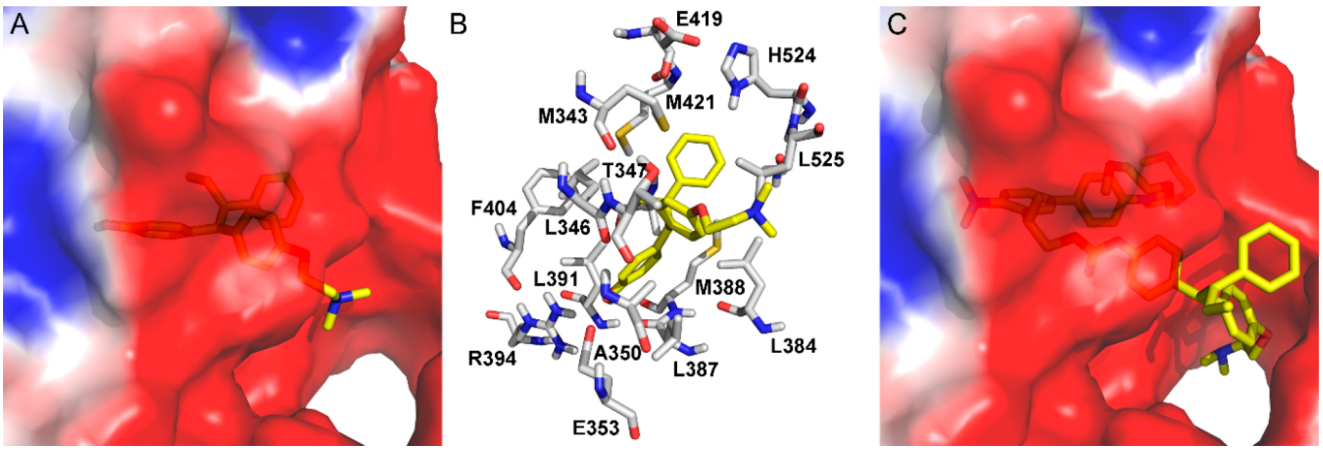

Figure 3. Molecular docking analyses. (A) Binding of 4-OHT (yellow) in the binding pocket. (B) Residues of hER interacting with 4-OHT. (C) Binding of EANBP-4-OHT (yellow) in the binding pocket. Note that the 4-OHT motif could not bind to the same binding site as shown in (A). The protein is represented as an electrostatic surface (red for negative electrostatic potential and blue for positive electrostatic potential).

CreERT2 fusion protein[25] under control of the astrocytic GFAP promoter[27] in addition to harboring (ii) a Cre-dependent tdTomato construct ("Ai14") for tamoxifen-inducible tdTomato expression.[28] Incubation of slices with 10 μM EANBP-4-OHT for 2 h followed by 20 s of irradiation induced substantial tdTomato expression (Figure 4A)

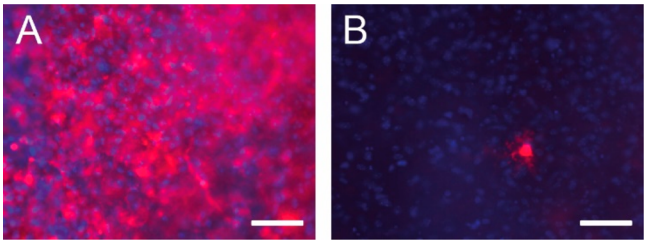

Figure 4. *Ex vivo* photoactivation of EANBP-4-OHT induced tdTomato expression in hippocampal brain slices of GFAP-CreERT2:Ai14 mice. (A) Irradiation of slices through a DAPI filter set produced widespread tdTomato expression (red; DAPI stain in blue). (B) Without irradiation, only a few astrocytes were tdTomato-positive. Scale bars: 50 μm.

compared to controls. Slices that were incubated with caged 4-OHT but were not irradiated only exhibited sporadic tdTomato fluorescence indicative of minor thermal hydrolysis of EANBP-4-OHT (Figure 4B).

With the possibility of a future application of photoactivated transgene expression in human eyes, the delivery of (caged) 4-OHT to the retina should be efficiently achieved with standard patient interventions. We therefore first tested different routes of 4-OH tamoxifen administration, including direct intravitreal injections into the eyes, topical application in form of eye drops, or intraperitoneal (ip) injections. The administration routes were tested with the GFAP-CreERT2:Ai14 mice or by targeting endothelial cells with the Tie2 promoter[3] (Tie2-CreERT2:Ai14). The most intense transgene expression was observed by intravitreal injections, while topical administration of 4-OHT *via* eye drops produced spotty, good expression and IP injections showed a uniformly weaker tdTomato signal (Figure S4). We took advantage of direct injections into eyes and the only small quantities of (caged) 4-OHT required for high transgene expression. For *in vivo* photoactivation, we used the same epifluorescence microscope and filter settings as with the *ex vivo* slices. We initially established the *in vivo* photoactivation procedure with a caged fluorescein derivative (CMNB-caged carboxyfluorescein) and found that 1 min of intermittent irradiation successively increased the fluorescein signal in the eye. Subsequent retina mounting revealed a distinct region of photoactivated fluorescence (Figure S5).

Using these irradiation parameters also for *in vivo* photoactivation, we achieved induction of tdTomato expression in endothelial cells of the retinal vasculature of Tie2-CreERT2:Ai14 double transgenic mice (Figure 5A). Compared to

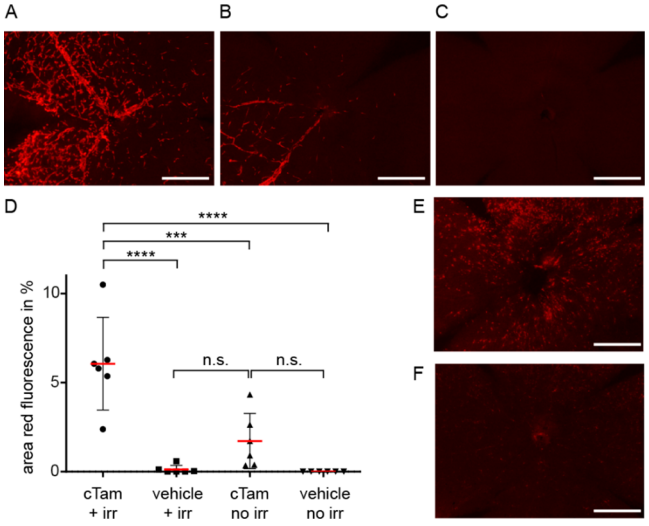

Figure 5. *In vivo* photoactivation induced tdTomato expression in retinas. (A, B) Example images of retinas from eyes of Tie2-CreERT2:Ai14 mice injected with EANBP-4-OHT (cTam) followed by irradiation (irr) (A) or without irradiation (no irr) (B). (C) Retina of control eye that was injected with vehicle only and not irradiated. (D) Each data point represents one retina, and for each of the four conditions, six mice were used (n = 6). Control injections without caged tamoxifen did not produce any tdTomato signal. Irradiation of eyes injected with caged tamoxifen increased tdTomato fluorescence in the retinal vasculature (percent area tdTomato fluorescence of total retinal area) compared to unirradiated eyes (one-way ANOVA, multiple comparisons, $P < 0.0001$). (E, F) Example images of retinas from eyes of GFAP-CreERT2 mice injected with EANBP-4-OHT (cTam) followed by irradiation (E) or without irradiation (F).

https://doi.org/10.1021/jacsau.4c00434
JACS Au 2024, 4, 2818−2825

unirradiated eyes that were injected with EANBP-4-OHT, photoactivation increased tdTomato expression (Figure 5B). Eyes injected with vehicle only did not show any expression (Figure 5C). Photoactivation of EANBP-4-OHT reproducibly led to significant increases of tdTomato above levels from unirradiated but injected as well as vehicle-injected eyes (Figure 5D). We believe that the limited tdTomato expression in unirradiated, injected control eyes is due to a combination of residual transcriptional activity of EANBP-4-OHT and hydrolysis of EANBP-4-OHT. Notably, the irradiation protocol did not induce retinal apoptosis, as independently verified with control *in vivo* irradiated eyes (Figure S6). To demonstrate that the method of photoactivated transgene expression can be flexibly used in multiple genetic backgrounds, we conducted another set of experiments with double transgenic GFAP-CreERT2:Ai14 mice. After injection of EANBP-4-OHT and subsequent irradiation of eyes, we again observed substantial tdTomato expression due to optogenetic induction (Figure 5e) compared to unirradiated eyes (Figure 5f). We concluded that retinal transgene expression can be induced upon photoactivation of EANBP-4-OHT in different genetic backgrounds and with high efficiency, as five of six retinas exhibited tdTomato expression above levels seen in unirradiated but EANBP-4-OHT-injected eyes (Figure 5d).

DISCUSSION

The method of "optogenetics", *i.e.*, the expression of light-sensitive ion channels for manipulation of ion currents, is increasingly being used for restoration of vision loss in patients with photoreceptor damage.[29,30] We envision expanding the therapeutic repertoire for light-mediated manipulation of retinal tissue by introducing photoinducible transgene expression. Genetic interference is a powerful tool to augment cellular function in retinal pathologies, but all current approaches lack the possibility to spatially target antiangiogenic gene therapies specifically to pathological regions of the retina. Merging existing gene therapies with photoactivated gene expression will solve this problem. In the preliminary phase of such a treatment concept, we showed here in proof-of-principle experiments the feasibility of using light to acutely manipulate cellular processes in the living eye.

Light-sensitive gene therapies based on conditional transgene expression paradigms such as the Cre/lox or Tet system will always depend and be limited by the cellular specificity provided by the exogenous promoter, such as the GFAP and Tie2 promoters used in this study. Notably, photoactivation substantially reduces potential off-target effects by restricting transgene expression to irradiated areas. Our goal is ultimately to be able to target photoactivated transgene expression to predetermined areas of the retina by regionally restricted irradiation using the optical properties of the eye. While the cornea and lens absorb much of UV irradiation, visible light above 400 nm readily reaches the most posterior layers of the retina. We therefore believe that shifting photoactivation wavelengths more to the visible spectrum will improve the efficacy of the method. Nevertheless, possible retinal phototoxicities[31] will be a key issue going forward, although photoactivation will be spatially restricted to pathological regions. Also, we[32] and others[33,34] have recently developed photoremovable protecting groups with high uncaging quantum yields so that a high light sensitivity of the method will ensure less photoactivation exposure and consequently less phototoxicity. Overall, we were encouraged by the high *ex vivo* and *in vivo* transgene induction efficiency as well as the ease of handling with our approach. In the future, these findings will have to be substantiated by in-depth characterization of the retina and vision function following photoactivation of antiangiogenic transgenes as well as by assessing the overall safety of the approach in animal models of pathological neovascularization. Further optimization of gene therapies to improve regulation and persistence of viral transgene expression as well as potential immune responses against the viruses can be readily accommodated with our photoactivation method.

Increasing chemical stability and using ophthalmoscopes with sophisticated adaptive optics in the future will clearly improve the spatial resolution, handling, and efficiency of our method. Here we demonstrated reproducible photoactivation of caged 4-OHT in two different genetic backgrounds by global irradiation of eyes with a standard epifluorescence microscope. For this, we synthesized EANBP-4-OHT, which can be efficiently uncaged in the visible range between 420 and 450 nm. Also, compared to previously published photosensitive tamoxifen analogs, EANBP-4-OHT is predicted to have a higher two-photon uncaging cross section for possible two-photon uncaging.[35]

Finally, we used an inducible transgene expression method based on a small diffusible molecule because tamoxifen analogs can be washed in and out of patients in a possible treatment scenario. After photoactivation and subsequent 4-OHT washout, therapeutic viral gene constructs allowing induction of Cre-dependent antiangiogenic transgenes would be insensitive to incoming light. Photoactivated transgene expression based on a light-sensitive analog of tamoxifen, which is currently approved by the FDA to treat breast cancer, is therefore expected to be applicable for future treatments in human eyes.

METHODS

EANBP-4-OHT Synthesis

The reagents used for the synthesis were ordered from Sigma-Aldrich, ABCR, Acros Organics, or Alfa Aesar. All commercial reagents were used without any further purification before use, except for dichloromethane (distilled over CaH_2 under an argon atmosphere) and THF (distilled over sodium/benzophenone under an argon atmosphere).

^1H and ^{13}C NMR spectra were recorded at 400 and 100 MHz using the following Bruker NMR instruments: a 400 MHz spectrometer equipped with an Avance III console and a BBO H/F *z*-gradient probe. Chemical shifts (δ) are indicated in parts per million with respect to the NMR solvent residual signal ($CDCl_3$: 7.26 ppm). The attributions are given in the following manner: chemical shift (multiplicity, coupling constant, number of protons). Multiplicities are denoted as br, d, t, q, and m, corresponding respectively to singlet, broad, doublet, triplet, quadruplet, and multiplet.

The LC-MS spectra were measured using an Agilent LC 1200 series/QToF 6520 spectrometer. The LC system was run using a ZORBAX RRHD SB-C18 2.1 mm i.d. × 50 mm, 1.8 μm threaded column and acetonitrile + 0.05% formic acid/Milli-Q H_2O + 0.05% formic acid as the elution system. Spectra were acquired by positive-mode electrospray ionization (ESI+) (T_{source} = 340 °C, V_{cap} = 4000 V). Thin-layer chromatography (TLC) analyses were realized using aluminum plates covered with silica gel 60 F254 (Merck). Column chromatography was done with silica gels (230−400 mesh, 0.040−0.063 mm, Merck). Some purifications were performed using TLC plates from Miles Scientific (silica gel GF, UV254, 20 cm × 20 cm, 1500 μm).

https://doi.org/10.1021/jacsau.4c00434
JACS Au 2024, 4, 2818−2825

HPLC purifications were realized using a Waters HPLC system, including a Waters 600 double body pump with a Waters 2996 detector and a Thermo Betabasics 5 μm (10 mm, 250 mm) column. The HPLC purifications were done using an isocratic mode of 80% Milli-Q H_2O acidified with 0.01% TFA and 20% acetonitrile.

Synthetic Procedure

To a cold solution of 2-(4′-(bis(2-(2-methoxyethoxy)ethyl)amino)-4-nitro-[1,1′-biphenyl]-3-yl)propan-1-ol (74 mg, 2 equiv) dissolved in anhydrous THF (3 mL) in an ice−water bath were added DIPEA (25.6 μL, 2 equiv) and triphosgene (46 mg, 2 equiv). The mixture was stirred at 0 °C for 3 h and then concentrated in vacuo. The residue was dissolved in anhydrous CH_2Cl_2 (3 mL), and DIPEA and 4-OHT (30 mg, 1.0 equiv) were added dropwise. Then DMAP (25 mg, 2 equiv) was added to the solution at 20 °C. This mixture was stirred at reflux for 19 h in the dark and evaporated to dryness. The residue was purified by semipreparative HPLC (RP-HPLC C18 using a mixture of solvent A (TFA (0.1%) in H_2O) and solvent B (acetonitrile), 80−20%; flow rate 4 mL/min^{-1}, t_R = 13 min) to afford 14 mg of EANBP-4-OHT (20% yield) as a yellow oil.

^{1}H NMR (500 MHz, $CDCl_3$): δ = 7.92 (d, ^3J(H,H) = 8.8 Hz, 1H), 7.61 (d, ^4J(H,H) = 4.0 Hz, 1H), 7.54−7.49 (m, 3H), 7.20−7.08 (m, 9H), 6.81 (d, ^3J(H,H) = 8.0 Hz, 2H), 6.77 (d, ^3J(H,H) = 8.0 Hz, 2H), 6.52 (d, ^3J(H,H) = 8.4 Hz, 2H), 4.48 (t, ^3J(H,H) = 7.8 Hz, 2H), 4.23 (br s, 2H), 3.66−3.47 (m, 16H), 3.48 (t, ^3J(H,H) = 7.8 Hz, 1H), 3.39 (s, 6H), 2.86 (s, 6H), 2.85 (s, 2H), 2.44 (q, ^3J(H,H) = 7.5 Hz, 2H), 2.34 (t, ^3J(H,H) = 7.8 Hz, 2H), 1.48 (d, ^3J(H,H) = 7.8 Hz, 6H), 0.97 (t, ^3J(H,H) = 7.5 Hz, 2H) ppm. ^{13}C NMR (101 MHz, $CDCl_3$): δ = 155.24, 153.74, 151.65, 149.88, 148.51, 147.68, 146.15, 142.68, 142.12, 141.39, 137.80, 136.96, 136.85, 135.92, 132.30, 130.58, 129.71, 128.42, 128.09, 126.40, 126.08, 125.72, 125.64, 124.88, 120.86, 113.52, 112.26, 72.47, 72.10, 70.79, 68.51, 62.64, 59.23, 56.41, 43.63, 34.36, 33.53, 30.46, 17.99, 13.62 ppm. See Figure S7 for the NMR spectra.

MS (ESI): $[M + 2H]^{2+}$ ($C_{51}H_{62}N_3O_{10}^{2+}$) m/z calculated 445.73, found 445.65.

Molecular Docking

The interactions of 4-OHT and EANBP-4-OHT with hER were investigated by molecular docking. The crystal structure of the ligand-binding domain of hER bound with 4-OHT (PDB ID 3ERT)[36] was used to model the receptor. In line with the experimental data,[25] triple mutations (G440V, M543A, and L544A) were introduced to the hER structure. AutoDock Vina[23] was used to perform molecular docking. To prepare the docking input files, the hER structure was represented with CHARMM36m force field parameters,[37] and the ligands (4-OHT and EANBP-4-OHT) were represented with the CHARMM general force field parameters.[38] The web server CHARMM-GUI[39] was used to generate the required input files for the receptor and ligands. The geometrical center of the 4-OHT in the crystal structure was used determine the searching space with a boundary 20 Å from the center. For each ligand, the binding pose with the best docking score was selected for structural analysis and binding affinity (binding energy) calculations.

One-Photon Photolysis

A 2 mL solution of compound EANBP-4-OHT (at 50 μM) in ACN/0.1 M PBS buffer (pH 7.1, 1:1 v/v) at 20 °C was exposed to an LED light source (LUMOS 43 LED; Atlas Photonics Inc.) using the 405 nm irradiation mode with a standard optical output of about 200 mW/cm^2. The photolysis reaction was monitored by UV−vis spectroscopy, and aliquots of samples (100 μL) were analyzed by HPLC, leading to the quantification of 52% 4-OHT release after 17 min of photolysis by using a 4-OHT HPLC calibration curve.

Stability toward Hydrolysis of EANBP-4-OHT in the Dark

The stability of our compound toward hydrolysis in the dark was assessed by HPLC monitoring of 55 μM solutions in ACN/0.1 M PBS buffer (pH 7.1, 1:1 v/v) over 2 days at room temperature (20 °C).

Determination of the Photochemical Quantum Yield

The quantum yield for the photoconversion was determined in ACN/0.1 M PBS buffer (pH 7.1, 1:1 v/v) by comparison with EANBP-GABA reported by Donato et al. (Φ_{ref} = 0.15)[19] at the same concentration (50 μM) as reference. For the light source, a LUMOS 43 LED equipment (from Atlas Photonics Inc.) was used in the 405 nm irradiation mode (typical optical output: 200 mW/cm^2). The reaction was monitored by UV spectroscopy on 2 mL of a 50 μM solution of EANBP-4-OHT. To determine the extent of the photolytic conversions, difference spectra ($t_{irr} - t_0$) were used. Full photolysis was confirmed by HPLC analysis. The absorbance evolution at 400 nm (for EANBP-GABA reference molecule and EANBP-4-OHT) was plotted to follow the uncaging kinetics (k_{sample} for EANBP-4-OHT and k_{ref} for the EANBP-GABA reference molecule), and the values were normalized. According to the following equation, the ratio of the rate constants was indeed directly proportional to the one-photon uncaging sensitivities of the new compound ($\varepsilon_{sample\ at\ 405\ nm} \times \Phi_{sample}$) and the reference compound ($\varepsilon_{ref\ at\ 405\ nm} \times \Phi_{ref}$):

$$\frac{k_{sample}}{k_{ref}} = \frac{\varepsilon_{sample} \times \Phi_{sample}}{\varepsilon_{ref} \times \Phi_{ref}} \quad (1)$$

Notably, the ε values at the excitation wavelength of EANBP-4-OHT and the EANBP-GABA reference molecule were equal in this experiment.

Transgenic Animals

All experiments were conducted in accordance with the German animal welfare guidelines and were approved by the Regierungspräsidium Karlsruhe (G-218/15; G-112/19; T-34/21) and the Regierungspräsidium Darmstadt (FU/2058). Mice were kept at a 12 h/12 h dark/light cycle synchronized with the local day/night cycle. Water and food were available *ad libitum*. Mice were housed in ventilated racks with up to three animals per cage but were separated after surgery to minimize the risk of injury and to prevent transfer of (caged) 4-OHT between mice. Three transgenic mouse lines were used: the "Tie2-CreERT2" line for expression in vascular endothelial cells (TgN(Tie2CreERT2)1399Gsc),[3] the "GFAP-CreERT2" line for astrocytic expression of CreERT2 (TgN(GFAP-CreERT2)),[27] and the "Cre-dependent tdTomato" line Ai14 (B6-Gt(ROSA)26Sortm14-(CAG-tdTomato)Hze).[28] Mice were genotyped using standard PCR protocols.

In Vivo Photoactivation

Photoactivated transgene expression *in vivo* in the retina was conducted with double transgenic, double homozygous Tie2CreER-T2:Ai14 or GFAP-CreERT2:Ai14 mice. Adult mice were anesthetized by intraperitoneal injection with a "sleep mix" of fentanyl (0.05 mg/kg mouse body weight), midazolam (5 mg/kg), and metedomidin (0.5 mg/kg). The sleep mix could be antagonized with a subcutaneous injection of atipamezol (750 μg/kg), flumazenil (0.5 mg/kg), and naloxon (1.2 mg/kg). Before intravitreal injection, mydriatic eye drops were applied (Neosynephrin-POS 5%, Ursapharm), and topical analgesia was provided through eye drops (Xylocain 1%, AstraZeneca). To prevent drying out of eyes in between treatment and irradiation, eyes were covered with Bepanthen (Bayer, 5% dexpanthenol). Using a 35G fine needle connected to a 10 μL syringe (NF35BV-2+ NanoFil; World Precision Instruments) under a standard stereomicroscope, eyes were intravitreally injected with a volume of 1 μL. Caged tamoxifen was dissolved in DMSO at a concentration of 10 mM for the Tie2 group and at 0.3 mM for the GFAP group. Following intravitreal injection, mice were kept for 3 h in the dark on a 37 °C heating plate. We used an upright epifluorescence microscope (Zeiss) and excitation light coming through a standard DAPI filter set for uncaging at 365 ± 20 nm. Intermittent photoactivation was performed in mydriasis using a 10× air objective for a total irradiation time of 1 min. Eyes were irradiated by alternating 10 s light exposure with 10 s pause for a total of six cycles. The irradiation pattern was based on pilot uncaging experiments with CMNB-caged carboxyfluorescein, SE (Invitrogen)

https://doi.org/10.1021/jacsau.4c00434
JACS Au 2024, 4, 2818−2825

dissolved in DMSO (5 mM); we injected 1 μL of the caged dye into eyes.

Following *in vivo* photoactivation of caged 4-OHT and antagonization of anesthesia, mice were returned to their cages and sacrificed 4 days after treatment. Eyes were collected and fixed for 1 h in 4% PFA, and retinas were removed for standard mounting. After retina isolation following wholemount preparation, incisions were made to create four roughly evenly sized retinal tissue sections, and the whole preparation was subsequently mounted with mounting medium (VECTASHIELD HardSet Antifade H-1400-10) on a slide. Each retina was subdivided into five image regions, and the expressed tdTomato signal was averaged across all regions. The color threshold function of ImageJ was used to generate a coefficient of the fluorescent area and the total retinal area. The thresholds were set for each retina separately to reduce the bias of fluorescence artifacts. The quantification was done blindly. Control experiments to test for apoptosis after irradiation were performed with a TUNEL (TdT-mediated dUTP Nick-End Labeling) assay kit (Promega) according to the manufacturer's instructions.

Ex Vivo Slice Cultures

Postnatal day 1 organotypic hippocampal cultures (OTCs) of double transgenic mice (GFAP-CreERT2:Ai14) were prepared according to standard procedures.[26] Briefly, whole brains were cut into 300 μm thick slices with a vibratome (Leica) and placed on a membrane filter (Millipore Millicell Cell Culture Insert, 30 mm, hydrophilic PFTE, 0.4 μm). EANBP-4-OHT in DMSO was administered to final concentration of 10 μM by adding it directly into the medium 3 days after preparing the slices, followed by incubation for 2 h in the dark. Before photoactivation, membranes with the hippocampal cultures were washed for a few seconds in medium without EANBP-4-OHT, and the tissues were immediately irradiated. We used the same upright epifluorescence microscope equipped with a 10× air objective and a standard DAPI filter set for *in vivo* eye experiments and the *ex vivo* OTC experiments. The length of irradiation was again determined in control experiments with caged fluorescein, which indicated that photolytic release saturated after 15−20 s; photoactivations for this length of time were subsequently used. After irradiation, slices on inserts were placed in fresh medium and returned to the incubator under normal conditions for 1 day in the dark. Slices were then fixed for 5 min in 4% PFA and counterstained for DAPI.

■ ASSOCIATED CONTENT

Supporting Information

The Supporting Information is available free of charge at https://pubs.acs.org/doi/10.1021/jacsau.4c00434.

Additional biological control experiments (PDF)

■ AUTHOR INFORMATION

Corresponding Authors

Alexandre Specht − *Laboratoire de Chémo-Biologie Synthétique et Thérapeutique, Equipe Nanoparticule Intelligentes, Université de Strasbourg, CNRS, CBST UMR 7199, F-67000 Strasbourg, France;* orcid.org/0000-0001-5056-5278; Email: specht@unistra.fr

Sidney Cambridge − *Dr. Senckenberg Anatomy, Anatomy II, Goethe-University Frankfurt, 60590 Frankfurt am Main, Germany; Department of Medicine, Health and Medical University Potsdam, 14471 Potsdam, Germany;* orcid.org/0000-0002-6438-4037; Email: cambridge@med.uni-frankfurt.de

Authors

Eric Brandhorst − *Fifth Medical Department, Medical Faculty Mannheim, University of Heidelberg, 68167 Mannheim, Germany*

Liang Xu − *Division of Bioinformatics and Biostatistics, National Center for Toxicological Research, U.S. Food and Drug Administration, Jefferson, Arkansas 72079, United States;* orcid.org/0000-0002-6556-7521

Maxime Klimezak − *Laboratoire de Chémo-Biologie Synthétique et Thérapeutique, Equipe Nanoparticule Intelligentes, Université de Strasbourg, CNRS, CBST UMR 7199, F-67000 Strasbourg, France*

Bastien Goegan − *Laboratoire de Chémo-Biologie Synthétique et Thérapeutique, Equipe Nanoparticule Intelligentes, Université de Strasbourg, CNRS, CBST UMR 7199, F-67000 Strasbourg, France*

Huixiao Hong − *Division of Bioinformatics and Biostatistics, National Center for Toxicological Research, U.S. Food and Drug Administration, Jefferson, Arkansas 72079, United States;* orcid.org/0000-0001-8087-3968

Hans-Peter Hammes − *Fifth Medical Department, Medical Faculty Mannheim, University of Heidelberg, 68167 Mannheim, Germany*

Complete contact information is available at: https://pubs.acs.org/10.1021/jacsau.4c00434

Author Contributions

E.B. performed the biological experiments, L.X. and H.H. had ideas on the modeling analyses and provided the interpretation of modeling results, B. G. and M. K. contributed to the caged 4-OH tamoxifen synthesis and characterization, H.P.H. contributed to the biological experiments, A.S. synthesized the caged 4-OH tamoxifen and wrote the manuscript, S.B.C designed the study and wrote the manuscript. All authors contributed to the editing of the manuscript. CRediT: **Eric Brandhorst** data curation, formal analysis, investigation; **Liang Xu** conceptualization, formal analysis, investigation, methodology; **Bastien Goegan** investigation, methodology; **Huixiao Hong** conceptualization, supervision, validation; **Hans-Peter Hammes** resources, supervision; **Alexandre SPECHT** conceptualization, funding acquisition, methodology, project administration, resources, supervision, writing-original draft; **Sidney Boris Cambridge** conceptualization, funding acquisition, investigation, methodology, project administration, supervision, validation, visualization, writing-original draft, writing-review & editing.

Notes

This article reflects the views of the authors and does not necessarily reflect those of the U.S. Food and Drug Administration.

The authors declare no competing financial interest.

■ ACKNOWLEDGMENTS

We thank Antonio Ortiz for help with the illustration, Frank Kirchhoff for providing the GFAP-CreERT2 line, and Markus Hecker for providing the Tie2-CreERT2 line. E.B. was supported by a grant from the Deutsche Diabetes Gesellschaft. A.S. acknowledges support by the Agence Nationale de la Recherche (Contract No. ANR-13-JSJV-0009-01).

■ ABBREVIATIONS

VEGF, vascular endothelial growth factor; 4-OHT, 4-hydroxytamoxifen; EANBP, 2-(4′-(bis(2-(2-methoxyethoxy)-ethyl)amino)-4-nitro-[1,1′-biphenyl]-3-yl)propan-1-ol; hER, human estrogen receptor; FDA, U.S. Food and Drug

https://doi.org/10.1021/jacsau.4c00434
JACS Au 2024, 4, 2818−2825

Administration; DAPI, 4′,6-diamidin-2-phenylindole; GFAP, glial fibrillary acidic protein

REFERENCES

(1) Campbell, M.; Doyle, S. L. Current perspectives on established and novel therapies for pathological neovascularization in retinal disease. *Biochem. Pharmacol.* **2019**, *164*, 321−325.

(2) Campochiaro, P. A. Ocular neovascularization. *J. Mol. Med. (Berlin)* **2013**, *91* (3), 311−21.

(3) Forde, A.; Constien, R.; Grone, H. J.; Hammerling, G.; Arnold, B. Temporal Cre-mediated recombination exclusively in endothelial cells using Tie2 regulatory elements. *Genesis* **2002**, *33* (4), 191−7.

(4) Jin, K.; Zhu, Y.; Sun, Y.; Mao, X. O.; Xie, L.; Greenberg, D. A. Vascular endothelial growth factor (VEGF) stimulates neurogenesis in vitro and in vivo. *Proc. Natl. Acad. Sci. U. S. A.* **2002**, *99* (18), 11946−50.

(5) Cambridge, S. B.; Davis, R. L.; Minden, J. S. Drosophila mitotic domain boundaries as cell fate boundaries. *Science* **1997**, *277* (5327), 825−8.

(6) Cambridge, S. B.; Geissler, D.; Keller, S.; Curten, B. A caged doxycycline analogue for photoactivated gene expression. *Angew. Chem., Int. Ed.* **2006**, *45* (14), 2229−31.

(7) Goegan, B.; Terzi, F.; Bolze, F.; Cambridge, S.; Specht, A. Synthesis and Characterization of Photoactivatable Doxycycline Analogues Bearing Two-Photon-Sensitive Photoremovable Groups Suitable for Light-Induced Gene Expression. *ChemBioChem* **2018**, *19* (12), 1341−1348.

(8) Cambridge, S. B.; Geissler, D.; Calegari, F.; Anastassiadis, K.; Hasan, M. T.; Stewart, A. F.; Huttner, W. B.; Hagen, V.; Bonhoeffer, T. Doxycycline-dependent photoactivated gene expression in eukaryotic systems. *Nat. Methods* **2009**, *6* (7), 527−31.

(9) Sinha, D. K.; Neveu, P.; Gagey, N.; Aujard, I.; Benbrahim-Bouzidi, C.; Le Saux, T.; Rampon, C.; Gauron, C.; Goetz, B.; Dubruille, S.; Baaden, M.; Volovitch, M.; Bensimon, D.; Vriz, S.; Jullien, L. Photocontrol of protein activity in cultured cells and zebrafish with one- and two-photon illumination. *ChemBioChem* **2010**, *11* (5), 653−63.

(10) Feil, R.; Brocard, J.; Mascrez, B.; LeMeur, M.; Metzger, D.; Chambon, P. Ligand-activated site-specific recombination in mice. *Proc. Natl. Acad. Sci. U. S. A.* **1996**, *93* (20), 10887−90.

(11) Metzger, D.; Clifford, J.; Chiba, H.; Chambon, P. Conditional site-specific recombination in mammalian cells using a ligand-dependent chimeric Cre recombinase. *Proc. Natl. Acad. Sci. U. S. A.* **1995**, *92* (15), 6991−5.

(12) Lerch, M. M.; Hansen, M. J.; van Dam, G. M.; Szymanski, W.; Feringa, B. L. Emerging Targets in Photopharmacology. *Angew. Chem., Int. Ed.* **2016**, *55* (37), 10978−99.

(13) Faal, T.; Wong, P. T.; Tang, S.; Coulter, A.; Chen, Y.; Tu, C. H.; Baker, J. R.; Choi, S. K.; Inlay, M. A. 4-Hydroxytamoxifen probes for light-dependent spatiotemporal control of Cre-ER mediated reporter gene expression. *Mol. BioSyst.* **2015**, *11* (3), 783−90.

(14) Shi, Y.; Koh, J. T. Light-activated transcription and repression by using photocaged SERMs. *ChemBioChem* **2004**, *5* (6), 788−96.

(15) Wong, P. T.; Roberts, E. W.; Tang, S.; Mukherjee, J.; Cannon, J.; Nip, A. J.; Corbin, K.; Krummel, M. F.; Choi, S. K. Control of an Unusual Photo-Claisen Rearrangement in Coumarin Caged Tamoxifen through an Extended Spacer. *ACS Chem. Biol.* **2017**, *12* (4), 1001−1010.

(16) Klimezak, M.; Chaud, J.; Brion, A.; Bolze, F.; Frisch, B.; Heurtault, B.; Kichler, A.; Specht, A. Triplet-Triplet Annihilation Upconversion-Based Photolysis: Applications in Photopharmacology. *Adv. Healthcare Mater.* **2024**, DOI: 10.1002/adhm.202400354.

(17) Morville, C.; Chaud, J.; Bolze, F.; Specht, A. Photolytical reactions for light induced biological effectors release: on the road to the phototherapeutic window. *J. Inclusion Phenom. Macrocyclic Chem.* **2021**, *101* (3), 291−304.

(18) Weinstain, R.; Slanina, T.; Kand, D.; Klán, P. Visible-to-NIR-Light Activated Release: From Small Molecules to Nanomaterials. *Chem. Rev.* **2020**, *120* (24), 13135−13272.

(19) Herbivo, C.; Omran, Z.; Revol, J.; Javot, H.; Specht, A. Synthesis and characterization of cell-permeable caged phosphates that can be photolyzed by visible light or 800 nm two-photon photolysis. *ChemBioChem* **2013**, *14* (17), 2277−83.

(20) Donato, L.; Mourot, A.; Davenport, C. M.; Herbivo, C.; Warther, D.; Leonard, J.; Bolze, F.; Nicoud, J. F.; Kramer, R. H.; Goeldner, M.; Specht, A. Water-soluble, donor-acceptor biphenyl derivatives in the 2-(*o*-nitrophenyl)propyl series: highly efficient two-photon uncaging of the neurotransmitter γ-aminobutyric acid at λ = 800 nm. *Angew. Chem., Int. Ed.* **2012**, *51* (8), 1840−3.

(21) Jahn, H. M.; Kasakow, C. V.; Helfer, A.; Michely, J.; Verkhratsky, A.; Maurer, H. H.; Scheller, A.; Kirchhoff, F. Refined protocols of tamoxifen injection for inducible DNA recombination in mouse astroglia. *Sci. Rep.* **2018**, *8* (1), 5913.

(22) Eberhardt, J.; Santos-Martins, D.; Tillack, A. F.; Forli, S. AutoDock Vina 1.2.0: New Docking Methods, Expanded Force Field, and Python Bindings. *J. Chem. Inf Model* **2021**, *61* (8), 3891−3898.

(23) Trott, O.; Olson, A. J. AutoDock Vina: improving the speed and accuracy of docking with a new scoring function, efficient optimization, and multithreading. *J. Comput. Chem.* **2010**, *31* (2), 455−61.

(24) Sakkiah, S.; Selvaraj, C.; Guo, W.; Liu, J.; Ge, W.; Patterson, T. A.; Hong, H. Elucidation of Agonist and Antagonist Dynamic Binding Patterns in ER-alpha by Integration of Molecular Docking, Molecular Dynamics Simulations and Quantum Mechanical Calculations. *Int. J. Mol. Sci.* **2021**, *22* (17), 9371.

(25) Feil, R.; Wagner, J.; Metzger, D.; Chambon, P. Regulation of Cre recombinase activity by mutated estrogen receptor ligand-binding domains. *Biochem. Biophys. Res. Commun.* **1997**, *237* (3), 752−7.

(26) Stoppini, L.; Buchs, P. A.; Muller, D. A simple method for organotypic cultures of nervous tissue. *J. Neurosci Methods* **1991**, *37* (2), 173−82.

(27) Hirrlinger, P. G.; Scheller, A.; Braun, C.; Hirrlinger, J.; Kirchhoff, F. Temporal control of gene recombination in astrocytes by transgenic expression of the tamoxifen-inducible DNA recombinase variant CreERT2. *Glia* **2006**, *54* (1), 11−20.

(28) Madisen, L.; Zwingman, T. A.; Sunkin, S. M.; Oh, S. W.; Zariwala, H. A.; Gu, H.; Ng, L. L.; Palmiter, R. D.; Hawrylycz, M. J.; Jones, A. R.; Lein, E. S.; Zeng, H. A robust and high-throughput Cre reporting and characterization system for the whole mouse brain. *Nat. Neurosci* **2010**, *13* (1), 133−40.

(29) Sahel, J. A.; Boulanger-Scemama, E.; Pagot, C.; Arleo, A.; Galluppi, F.; Martel, J. N.; Esposti, S. D.; Delaux, A.; de Saint Aubert, J. B.; de Montleau, C.; Gutman, E.; Audo, I.; Duebel, J.; Picaud, S.; Dalkara, D.; Blouin, L.; Taiel, M.; Roska, B. Partial recovery of visual function in a blind patient after optogenetic therapy. *Nat. Med.* **2021**, *27* (7), 1223−1229.

(30) Yan, B.; Nirenberg, S. An Engineering Platform for Clinical Application of Optogenetic Therapy in Retinal Degenerative Diseases. *IEEE J. Transl Eng. Health Med.* **2023**, *11*, 296−305.

(31) Youssef, P. N.; Sheibani, N.; Albert, D. M. Retinal light toxicity. *Eye (Lond)* **2011**, *25* (1), 1−14.

(32) Chaud, J.; Morville, C.; Bolze, F.; Garnier, D.; Chassaing, S.; Blond, G.; Specht, A. Two-Photon Sensitive Coumarinyl Photoremovable Protecting Groups with Rigid Electron-Rich Cycles Obtained by Domino Reactions Initiated by a 5-exo-Dig Cyclocarbopalladation. *Org. Lett.* **2021**, *23* (19), 7580−7585.

(33) Lin, Q.; Yang, L.; Wang, Z.; Hua, Y.; Zhang, D.; Bao, B.; Bao, C.; Gong, X.; Zhu, L. Coumarin Photocaging Groups Modified with an Electron-Rich Styryl Moiety at the 3-Position: Long-Wavelength Excitation, Rapid Photolysis, and Photobleaching. *Angew. Chem., Int. Ed.* **2018**, *57* (14), 3722−3726.

(34) Shrestha, P.; Kand, D.; Weinstain, R.; Winter, A. H. meso-Methyl BODIPY Photocages: Mechanisms, Photochemical Properties, and Applications. *J. Am. Chem. Soc.* **2023**, *145* (32), 17497−17514.

(35) Boguslawski, J.; Palczewska, G.; Tomczewski, S.; Milkiewicz, J.; Kasprzycki, P.; Stachowiak, D.; Komar, K.; Marzejon, M. J.; Sikorski, B. L.; Hudzikowski, A.; Głuszek, A.; Łaszczych, Z.; Karnowski, K.;

https://doi.org/10.1021/jacsau.4c00434
JACS Au 2024, 4, 2818−2825

Soboń, G.; Palczewski, K.; Wojtkowski, M. In vivo imaging of the human eye using a 2-photon-excited fluorescence scanning laser ophthalmoscope. *J. Clin. Invest.* **2022**, *132* (2), e154218.
(36) Shiau, A. K.; Barstad, D.; Loria, P. M.; Cheng, L.; Kushner, P. J.; Agard, D. A.; Greene, G. L. The structural basis of estrogen receptor/coactivator recognition and the antagonism of this interaction by tamoxifen. *Cell* **1998**, *95* (7), 927−37.
(37) Huang, J.; Rauscher, S.; Nawrocki, G.; Ran, T.; Feig, M.; de Groot, B. L.; Grubmuller, H.; MacKerell, A. D., Jr. CHARMM36m: an improved force field for folded and intrinsically disordered proteins. *Nat. Methods* **2017**, *14* (1), 71−73.
(38) Vanommeslaeghe, K.; Hatcher, E.; Acharya, C.; Kundu, S.; Zhong, S.; Shim, J.; Darian, E.; Guvench, O.; Lopes, P.; Vorobyov, I.; Mackerell, A. D., Jr. CHARMM general force field: A force field for drug-like molecules compatible with the CHARMM all-atom additive biological force fields. *J. Comput. Chem.* **2010**, *31* (4), 671−90.
(39) Jo, S.; Kim, T.; Iyer, V. G.; Im, W. CHARMM-GUI: a web-based graphical user interface for CHARMM. *J. Comput. Chem.* **2008**, *29* (11), 1859−65.

https://doi.org/10.1021/jacsau.4c00434
JACS Au 2024, 4, 2818−2825